Stepwise synthesis of oligoamide coating on a porous support: Fabrication of a membrane with controllable transport properties

Stepwise synthesis of oligoamide coating on a porous support: Fabrication of a membrane with controllable transport properties

Paramita Manna[1], Alberto Tiraferri[2], Marco Sangermano[3], Roy Bernstein[1,*], and Roni Kasher[1,*]

[1]Department of Desalination and Water Treatment, Zuckerberg Institute for Water Research, Jacob Blaustein Institutes for Desert Research, Ben-Gurion University of the Negev, Midreshet Ben-Gurion, 8499000, Israel

[2]Department of Environment, Land and Infrastructure Engineering (DIATI), Politecnico di Torino, Corso Duca degli Abruzzi 24, 10129, Torino, Italy

[3]Department of Applied Science and Technology (DISAT), Politecnico di Torino, Corso Duca degli Abruzzi 24, 10129, Torino, Italy

[*]Corresponding authors; royber@bgu.ac.il (R.B.); kasher@bgu.ac.il (R.K.)

ABSTRACT

Porous polymeric membranes are widely used in potable water purification, wastewater treatment, the food and pharmaceutical industries, and haemodialysis. However, producing specialized membranes with diverse transport properties is challenging. A method for fabricating membranes with controllable transport properties is described here by stepwise synthesis of aromatic oligoamide on a porous polymeric support. The use of aromatic oligoamide affords good water permeance due to its hydrophilic character. Alternate couplings of trimesoyl chloride and meta-phenylenediamine yielded an oligoamide dendrimer that was covalently bonded to the support. The water permeance and molecular weight cutoff (MWCO) of the synthesized membranes were controlled (with values of 4.6 to 543 $L \cdot m^{-2} \cdot h^{-1} \cdot bar^{-1}$ and 22.6 to 332 kDa, respectively) by adjusting the number of oligoamide synthesis cycles in the range of 2.5 – 20.5. The oligoamide membrane with 5.5 synthetic cycles showed a high rejection of the negatively charged rose bengal dye (95% rejection) with high flux (126.4 ± 4.2 $L \cdot m^{-2} h^{-1}$ at 5.2 bar), as compared with other membranes reported in the literature. The fabricated membranes are potentially highly useful for the separation of macromolecules with specific ranges of molecular weight, for industrial separations that require membranes with tunable MWCO ranges, or for the separation of charged macromolecules.

Keywords: Stepwise synthesis; oligoamide; polyacrylonitrile; molecular weight cutoff; rose bengal separation.

1. Introduction

Water scarcity is a serious problem, and the shortage of fresh water worldwide is only expected to worsen in the coming decades [1]. Membrane processes are key technologies for wastewater treatment, desalination, and reduction of industrial waste, as well as for improving water-based industrial processes [2]. Methods to prepare porous membranes include phase inversion [3, 4], track-etching, stretching, and sintering [5-7], with phase inversion being the most widely applied and investigated. Dense nanofiltration (NF) and reverse osmosis (RO) membranes can either be prepared by phase inversion (asymmetric membranes), or by interfacial polymerization producing thin-film composite (TFC) membranes [8]. Other methods for producing TFC membranes include coating, grafting, and layer-by-layer deposition [9-13].

Nevertheless, new methods for fabricating advanced membranes with diverse transport properties and specialized performance are highly needed, and are a target of extensive research. For example, the self-assembly of block-polymers and template leaching have been used to prepare membranes with very narrow pore-size distributions and advanced performance [14]. The incorporation of organic and inorganic additives (such as nanoparticles) into the polymer casting solution during the phase inversion process may tune the pore size and morphology, and can alter the hydrophilic/hydrophobic properties of the membrane [15-18]. The surface charge of the membrane which can enhance the selectivity of charged solutes, can be varied by using chemically modified polymers (e.g., sulfonated polyphenyl sulfone) [19] or through surface grafting using charged monomers [20-22].

Aromatic polyamide is used successfully as a barrier film for reverse osmosis (RO) and nanofiltration (NF) dense membranes due to its hydrophilic character, which enables high water permeance, and due to its crosslinking propensity [23]. Nevertheless, its conventional preparation by interfacial polymerization limits the control of its thickness and crosslinking degree and hence its transport properties. Therefore, strategies of preparing polyamide films with controlled properties are explored. Karan *et al.* performed interfacial polymerization on a substrate having a sacrificial – intermediate layer obtaining a sub–10 nm polyamide film that was installed on ceramic support to obtain organic solvent nanofiltration composite membrane with high solvent permeances [24]. Chowdhury *et al.* used electro-spraying to deposit small droplet sizes of acid chloride and diamine monomers directly on a support and obtained reverse osmosis membranes with very thin polyamide films and controllable thicknesses [25].

A different approach was demonstrated by Steiner *et al.* (2011) [26] who synthesized an aromatic oligoamide on gold by a stepwise series of coupling reactions, where unlike the interfacial polymerization, a very thin oligoamide layer was formed and its thickness could be varied by the number of synthetic cycles. The stepwise approach of synthesizing aromatic oligoamide has recently been used by several research groups to fabricate novel polyamide membranes on porous supports. For example, Wu *et al.* used repeated layer-by-layer couplings of polyethyleneimine and trimesoyl chloride (TMC) on a polyethersulfone substrate [27] to make a membrane with permeability in the range of NF membranes. In another study, polyelectrolytes were pre-deposited on porous poly(acrylonitrile) membranes, then a stepwise preparation of aromatic polyamide barrier layer was successfully introduced [28, 29]. The resulting membranes performed similarly to aromatic polyamide NF membranes fabricated by conventional interfacial polymerization.

The recent studies described above used anchoring polymers between the porous substrate and the synthesized polyamide. Amelio *et al.* [30] recently used stepwise synthesis [26] to prepare an oligoamide layer covalently attached to an inorganic porous support. The synthesis was initiated by functionalization of alumina support with amino-silane groups, followed by stepwise assembly of TMC and meta-phenylenediamine (mPD); the water permeance and salt rejection of the resulting membrane were in the range of NF membranes.

Here, direct stepwise synthesis of aromatic oligoamide films on a porous polymeric support was studied for developing membranes with variable properties, which can be tuned through the preparation conditions. The choice of oligoamide was based on its hydrophilic character, which enables high water permeance, and its high stability. The oligoamide was covalently bonded to the support without an anchoring polymeric layer; as such, this type of membrane is expected to have high mechanical stability, which can be advantageous during backwash or operation under extreme conditions. To the best of our knowledge, this is the first report of stepwise synthesis of oligoamide film directly onto an organic porous support. Polyacrylonitrile (PAN) was chosen as the material of the support membrane because its functionalization with amine groups, which was needed for initiating the oligoamide synthesis, was feasible. A key challenge of developing the synthetic method was finding conditions compatible with the polymeric support; e.g., the correct choice of solvents. A series of membranes was prepared with different numbers of synthetic cycles, the physico-chemical properties of the membranes were characterized, and the water permeance, MWCO, and selectivity of the resulting membranes were determined.

2. Experimental Section

2.1. Materials

Powdered polyacrylonitrile (PAN; 150 kDa) and N-methyl-2-pyrrolidone (NMP) were supplied by Scientific Polymer Products (Ontario, NY, USA) and Bio lab (Jerusalem, Israel), respectively. Diethylenetriamine (DETA), polyethylene glycol (PEG), polyethylene oxide (PEO), mPD, TMC, sucrose, glucose, orange-II, rose bengal, triethanolamine, and 1,4-dioxane were purchased from Sigma Aldrich (St Louis, MO, USA). Sodium carbonate and sodium sulfate were purchased from Frutarom (Haifa, Israel). Except PEG and PEO, all chemicals were used as received. A dialysis tube (Sigma Aldrich, St Louis, MO; MWCO 14,000 Da) was used to purify the PEG of molecular weight higher than 35 kDa and PEO. Magnesium sulfate ($MgSO_4$) was purchased from Carlo Erba (Rodano, Italy). Commercial, flat-sheet, PAN membranes (Ultura^{TM} brand, Long Beach, CA, USA; MWCO 75 kDa) were mainly used as the supports for the fabrication of oligoamide membranes; otherwise, PAN membranes were cast in-house using non-solvent induced phase separation (see details below).

2.2. Membrane fabrication

2.2.1. Preparation of PAN membranes

A solution of 12% (w/w) PAN in NMP was prepared by stirring for 12 h with subsequent standing for 12 h to remove air bubbles. The membranes were cast on a poly(propylene) support by phase inversion, where double distilled water was used as the non-solvent in the coagulation bath. Membranes were stored in double-distilled water for 24 h before use.

2.2.2. Amination of the PAN membranes

PAN membranes were aminated using DETA (31%) as the amine in an aqueous solution (**Scheme 1**, Step 1) with 1% sodium carbonate [31]. The reaction was continued at a fixed temperature of 60 °C for different times (2–10 h). The degree of amination of the membranes was measured using orange-II staining (see below).

2.2.3. Stepwise synthesis of oligoamide membranes

Oligoamide membranes were synthesized as depicted in Scheme 1 (Steps II–IV), using aminated PAN membranes as the support for coupling alternately mPD and TMC [26]. The aminated PAN membranes were installed in a metallic dead-end filtration cell (porous disc of 38 mm diameter) and washed once with 1,4-dioxane for 10 min. The first cycle of synthesis was initiated by adding 40 mM solution of TMC in dioxane, and the reaction proceeded for 2 min with shaking on an orbital platform shaker (Heidolph Unimax 1010, Germany) at room temperature. Excess unreacted monomers were washed once for 2 min with dioxane on an orbital shaker; then, 5 mL 1,4-dioxane were filtered through the membranes by applying N_2 pressure, and the membranes were again washed for 1 min with 1,4-dioxane on the orbital shaker. Subsequently, 50 mM of mPD in dioxane was added into the cell, which was shaken for 2 min, and the membrane was subsequently washed again thoroughly with dioxane as described above. The successive TMC and mPD couplings (Steps II and III, Scheme 1) were repeated 1.5 (i.e., one time each, plus an additional Step II), 4.5 times, 9.5 times, 14.5 times, or 19.5 times, to perform 2.5, 5.5, 10.5, 15.5, and 20.5 reaction cycles, respectively, leading to membranes designated as OL-2.5, OL-5.5, OL-10.5, OL-15.5, and OL-20.5. Finally, the reaction was completed, including hydrolysis of the residual acyl chloride groups, by treatment in water at 50 °C for 15 min (IV, Scheme 1) and washing with water. The membranes were stored in water prior to use.

2.3. Chemical characterization

The degree of amination of the aminated PAN membranes was calculated by staining with orange-II dye [32]. The membranes were stained with 0.05 mM orange-II solution in HCl (pH 3) for 3 h, and rinsed with the HCl solution until the rinsing solution became colorless. Then, the adsorbed dye was eluted with a minimal volume of 30% (v/v) triethanolamine in water for 2 h. The absorbance of the dye was measured at 468 nm (UV-1800 spectrophotometer, Shimadzu) with reference to a 30% (v/v) triethanolamine solution. The concentration of the eluting solution was determined by using a calibration curve of orange-II dye in 30% (v/v) triethanolamine solution. The calculation of degree of amination was based on the membrane area, the volume of eluate, and the dye concentration of the eluting solution.

Surface functional groups of the oligoamide membranes were characterized by ATR-FTIR spectroscopy with a VERTEX 70-FTIR spectrometer (Bruker Optics, Ettlingen, Germany) at 4 cm^{-1} resolution. The system was equipped with a Miracle ATR attachment with a reflection

diamond-coated KRS-5 crystal (Pike, Madison, WI, USA). Before analyses, the membranes were dried in a vacuum oven at 40 °C. The IR analyses were performed in 3-4 different locations on each membrane sample, and the average spectra are reported.

Scanning electron microscopy (SEM) of surface topography and cross-sections of the membranes were performed with a Quanta 200 microscope (Field Electron and Ion Company, Thermo Fisher Scientific, USA). Cross-sectional SEM analyses were performed using OL-15.5 membranes synthesized on PAN supports cast in the lab (as described in Section 2.2.1), because the commercial PAN membranes did not allow cross-sectional analysis owing to their mechanical reinforcement. Surface topography SEM was performed using oligoamide membranes fabricated on commercial PAN membranes.

2.4. Membrane performance

Membrane performance tests were conducted using a dead-end filtration system with an effective membrane area of 11.34 cm^2 equipped with a magnetic stirrer.

Membrane permeability: The permeance of the membranes, L_p, was determined by measuring the permeate volume, divided by the time of collection of the permeate, the area of the membrane, and the pressure at which the measurement was carried out.

Rose Bengal separation: Separation of rose bengal dye (MW 973.67 g/mol; 1017.65 g/mol of the di-sodium salt) from water was conducted using the OL-2.5 and OL-5.5 membranes. Prior to dye filtration, the membranes were compressed by filtration with water at a constant pressure. Then, the filtration of rose bengal solution (20 µM) was conducted for 50 min with constant stirring. The concentration of rose bengal in the permeate and in the feed solutions was measured at 548 nm using UV-spectrophotometer (UV-1800, Shimadzu) and the rejection of rose bengal was calculated using Eq. (1), where C_p and C_f are the concentrations of permeate and feed, respectively. All the rejection and permeability data are the average of three different measurements.

$$\text{Rejection, R}\,(\%) = \left(1 - \frac{C_p}{C_f}\right) \times 100 \qquad (1)$$

Salt separation: The salt selectivity, expressed as the rejection rate (R), was evaluated by filtering 1 g/L solutions of Na_2SO_4 or $MgSO_4$, and measuring the feed and permeate conductivities upon reaching steady-state. The rejection rate was calculated by Eq. (2),

$$\text{Rejection, R}\,(\%) = \left(1 - \frac{\kappa_p}{\kappa_f}\right) \times 100 \qquad (2)$$

where κ_f and κ_p are the specific conductivities of the feed and permeate solutions, respectively.

Molecular weight cut-off (MWCO): The MWCO of each membrane was determined using glucose, sucrose, PEG (M_n 6 and 35 kDa), and PEO (M_n 100, 200, and 400 kDa) as molecular markers. Solutions of 100 mg/L of the molecular markers in Milli-Q water were prepared separately. The membranes were initially compacted with water. The solutions were then filtered through the membranes using a dead-end filtration system at pressures of 5–20 bar and under continuous stirring (500 rpm) to minimize the effect of concentration polarization. The concentrations of the molecular markers were determined in the feed and in the permeate upon reaching steady-state conditions. The concentration of the glucose and sucrose were determined by refractive index and Brix number measurements using a refractometer (Schmidt Haensch High Performance Refractometer, Texas, USA), whereas the concentrations of the macromolecules were determined by measuring the total organic carbon (TOC) concentrations of the feed and permeate solutions using a TOC analyzer (Multi N/C, 2100S, Analytikjena, Germany). For all markers, percentages of rejection were calculated according to Eq. (1) and plotted against the molecular weight of the marker. The MWCO for each membrane was determined from the resulting graph by extracting the molecular weight for 90% rejection.

2.5. Mean pore size calculation

The mean pore size of the membranes was estimated according to the study of S. Singh *et al.* [33]. Initially, the Stokes radii of the molecular markers were calculated using Eq. (3) for PEG and Eq. (4) for PEO

$$a = 16.73 \times 10^{-3}\, M_w^{0.557} \qquad (3)$$

$$a = 10.44 \times 10^{-3}\, M_w^{0.587} \qquad (4)$$

where *a* is the Stokes radius (nm) of the PEG or PEO, and M_w is the molecular weight (g/mol). The radius of glucose and sucrose molecules were taken as 0.38 and 0.5 nm, respectively.

By ignoring the steric and hydrodynamic interactions between the solute and membrane during separation [34, 35], the mean pore size and the geometric standard deviation of the membrane can be considered the same as the mean solute size and the solute geometric standard deviation. The solute rejection of each membrane was plotted against the solute

diameter, and the solute diameter that corresponded to 50% rejection was determined from the graph. The geometric standard deviation about the mean diameter was determined from the ratio of solute diameter at R = 84.13% to solute diameter at R = 50%.

3. Results and discussion

The oligoamide material was chosen for the stepwise synthesis coating due to its hydrophilic character, which enables high water permeance, and its stability. The stepwise synthesis was performed according to the procedure described in our previous study [26] of oligoamide synthesis on gold, where amine groups were used for the initial coupling stage. Hence, the fabrication of oligoamide on a porous support requires the substrate to have amine functionality. The porous supports used here were PAN ultrafiltration (UF) membranes, because they can be functionalized easily with primary amino groups through their reaction with polyamine compounds in a basic catalysis [31].

3.1. Amination of the PAN support

Amination was performed on the PAN membranes using DETA as the polyamine in aqueous sodium carbonate at elevated temperatures (Scheme S1, Supporting Information, and Scheme 1, Step 1). The reaction conditions were optimized by evaluating both the amine content and the permeance of the resulting aminated membranes. Comparing amination at 40, 60, and 80 °C showed that 60 °C resulted in similar amounts of amine groups as 80 °C, while the reaction at 40 °C yielded substantially lower amine density. The degree of amination of membranes prepared at 60 °C for different durations was also investigated, and is summarized in Table 1. The amine content after 2 h reaction (A2H, Table 1) was lower (1.094×10^{-4} mmol/cm^2) than after 5 or 10 h (1.501 and 1.561×10^{-4} mmol/cm^2, respectively). The 10 h-reaction membrane was substantially less permeable to water than all the others. Therefore, reaction at 60 °C for 5 h was chosen for the subsequent experiments, as it gave the most suitable combination of water permeance and degree of amination. The amination of PAN membranes reported earlier by Neghlani *et al.* [31, 36] used reactions at 90 °C. In the present study, we optimized the amination procedure to minimize membrane deterioration, finding that the reaction at 60 °C for 5 h yielded amine densities that were comparable to those formed at higher temperatures with 10 h reaction time.

Table 1. Water permeance and surface density of amine groups of PAN membranes aminated for different reaction times at 60 °C in the presence of DETA.

Support membrane	Reaction time (h)	Amine content[a] (mmole/cm^2)	Water permeance (L·m^{-2}h^{-1}bar^{-1})
PAN (Pristine)	0	3.86×10^{-6}	534.6±15.9
Aminated PAN (A2H)	2	1.094×10^{-4}	481.3±14.3
Aminated PAN (A5H)	5	1.501×10^{-4}	436.2±27.3
Aminated PAN (A10H)	10	1.561×10^{-4}	223.7±7.4

[a)]Measured by orange-II adsorption assay.

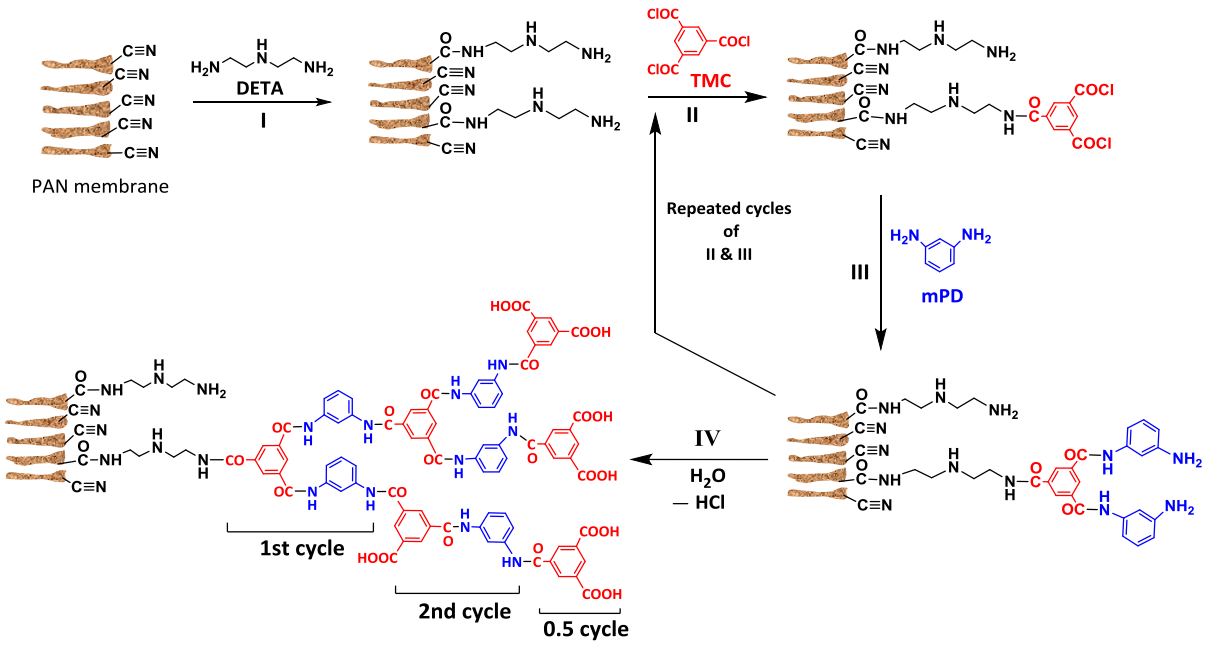

Scheme 1. Stepwise preparation of oligoamide on an amine functionalized porous PAN membrane, with detailed structure of oligoamide after 2.5 cycles. Step I: 31% diethylenetriamine (DETA) and 1% Na_2CO_3 in water at 60 °C. Step II: 40 mM trimesoyl chloride (TMC) in 1,4-dioxane, 2 min. III: 50 mM meta-phenylenediamine (mPD) in 1,4-dioxane, 2 min. Step IV: H_2O at 50 °C, 15 min.

3.2. Selection of suitable solvents for oligoamide synthesis on PAN

The choice of appropriate solvents for the oligoamide synthesis (Steps II and III, Scheme 1) was crucial: the solvent or solvents had to dissolve the monomers (TMC, mPD) while not degrading the membrane. The stepwise synthesis of oligoamide on gold reported by Steiner

et al. [26] and the recent work of coating oligoamide on alumina by Amelio *et al.* [30] used dimethylformamide (DMF) and dichloromethane (DCM) as the solvents for mPD and TMC, respectively. However, these solvents cannot be used here, as DMF and DCM dissolve most common polymers that are used for porous membranes preparation, including PAN membranes. The following solvents were identified as being compatible with PAN: toluene, hexane, water, and 1,4-dioxane. Table 2 lists the solubility of the monomers and the stability of PAN membrane in the four solvents, and thus shows that possible solvents for oligoamide synthesis are a combination of hexane or toluene for TMC, water for mPD, and toluene or 1,4-dioxane for both TMC and mPD. As washing between each step is important, a single solvent for both monomers is preferable with respect to synthesis with two immiscible solvents. Previous studies of molecular layer-by-layer approaches have used toluene [28, 29, 37], which does not dissolve TMC or mPD well. Given that the monomers were more soluble in 1,4-dioxane than in toluene (Table 2), 1,4-dioxane was chosen as the most suitable solvent for oligoamide synthesis in the present study.

Table 2. Comparison of solvents for oligoamide synthesis on PAN.

Solvent		mPD solubility[a]	TMC solubility	Permeance of PAN membrane ($L \cdot m^{-2} h^{-1} bar^{-1}$)	
				Before immersion	After immersion[b]
Hexane		NS	S	ND	ND
Toluene		PS	PS	ND	ND
Water		S	NS	ND	ND
1,4-dioxane/water solution	3:7	S	S	507.8	555.0
	6:4	S	S	500.5	540.9
	1:0	S	S	575.9	597.3

[a] PS, partially soluble; S, soluble; ND, not determined; NS, non-soluble.

[b] Immersion of the PAN membrane overnight in the solvent.

3.3. Oligoamide synthesis

Oligoamide synthesis was performed on the 5 h aminated PAN membrane as illustrated in Scheme 1, with both TMC and mPD dissolved in 1,4-dioxane. Successive TMC and mPD couplings (II and III, Scheme 1) were repeated to obtain oligoamide with 2.5, 5.5, 10.5, 15.5, and 20.5 synthesis cycles, including final hydrolysis (IV, Scheme 1) and extensive washing, and the membranes were designated as OL-2.5, OL-5.5, OL-10.5, OL-15.5, and OL-20.5. Although Steiner *et al.* [26] reported that their oligoamide synthesis on gold required organic base in the TMC reaction to neutralize the hydrochloric acid formed, we found that a base

was not essential for successful oligoamide synthesis on PAN membranes (see Table S1, Supporting Information). All the syntheses ended with TMC coupling (half a cycle), as carboxylic acid surface moieties make the membranes more hydrophilic than a typical amine–terminated surface. A possible structure for an oligoamide membrane with 2.5 synthetic cycles is shown in Scheme 1.

Surface functional groups on the membranes were characterized using ATR-FTIR spectroscopy (Fig. 1). All the vibrational spectra include a peak at 2244 cm^{-1}, which is characteristic of the nitrile stretching vibration of the PAN membrane. The aminated membranes displayed two new peaks at 1606 and 1572 cm^{-1} that are not shown by the pristine membrane; these peaks are characteristic of amine –N–H bending (see Supporting Information for the IR peaks of DETA). All the oligoamide membranes (2.5, 5.5, 10.5, 15.5, and 20.5 synthetic cycles) show new IR bands at 1655 (amide-I, C=O stretching vibration) and 1541 cm^{-1} (amide-II, N–H in-plane bending) that are attributed to the amide functionality of oligoamide [38]. Notably, the relative intensities of the amide-I and amide-II peaks increased with the number of synthetic cycles, as expected, owing to the increased size of the oligoamide. The peak at 1611 cm^{-1} is assigned to aromatic ring breathing, and both peaks at 1494 and 1453 cm^{-1} result from aromatic C=C stretching. The peak at 1306 cm^{-1} and the strong peak at 1251 cm^{-1} may be assigned to the C–N of amine and C–O stretching of carboxylic acid, respectively. No characteristic peak of acyl halide functionality (at 1770 cm^{-1}) was observed, indicating the negligible presence of unreacted acyl chloride groups. A peak at 1732 cm^{-1} was shown by the commercial PAN membranes (but those cast in the lab); this peak is characteristic of –C=O stretching in carboxylic acids or esters, and was probably due to additives present in the commercial membranes. Overall, the FTIR spectra show peaks typical of oligoamide on PAN, and the oligoamide peak intensities increased with increasing number of synthetic cycles as was expected from the stepwise synthesis.

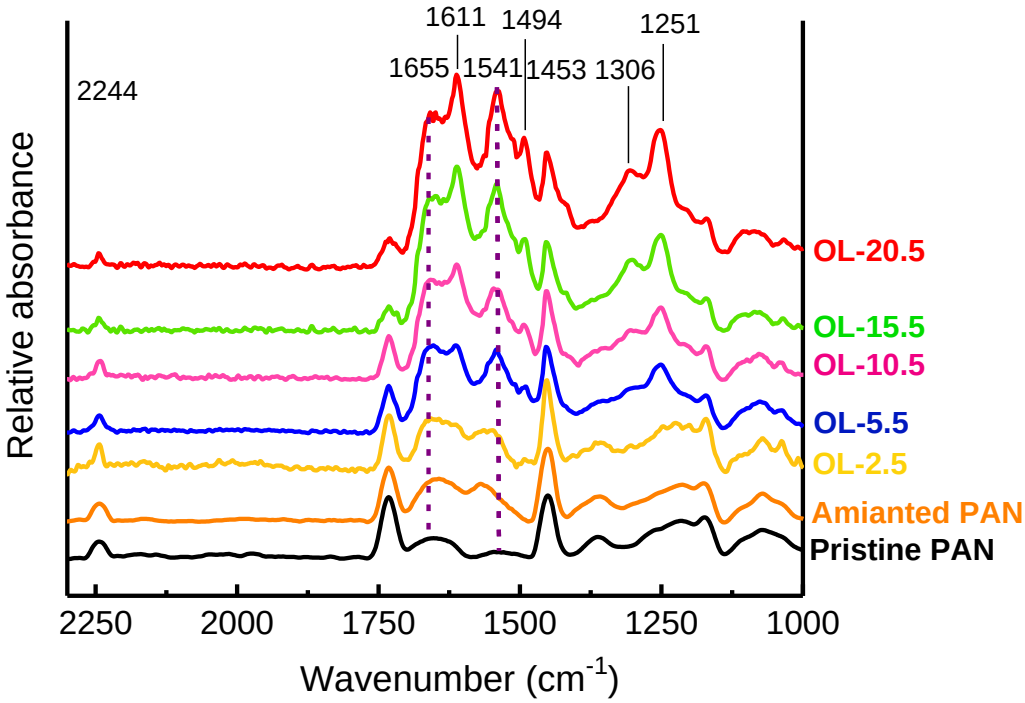

Figure 1. ATR-FTIR spectra of PAN-oligoamide membranes made by 2.5, 5.5, 10.5, 15.5, and 20.5 synthetic cycles (Scheme 1) alongside those of pristine PAN and aminated PAN membranes (A5H, Table 1).

3.4. Membrane transport properties

The synthesis of oligoamide on a porous PAN support is expected to produce membranes with diverse transport properties by reducing its permeability and pore size; therefore, the permeance was evaluated for membranes made with different numbers of oligoamide synthesis cycles (Fig. 2A). The pristine PAN membrane showed a water permeance of 543.4±9.0 $L \cdot m^{-2}h^{-1}bar^{-1}$, which was indeed greater than any permeance shown by the oligoamide membranes, whose values decreased with the number of cycles of oligoamide synthesis. The permeance significantly decreased after 2.5 cycles (OL-2.5 membrane) to 71.8±1.3 $L \cdot m^{-2}h^{-1}bar^{-1}$ and it decreased yet further to 4.6±0.2 $L \cdot m^{-2}h^{-1}bar^{-1}$ for the thickest membrane (OL-20.5). Fig. 2A also shows that the correlation between L_p and the number of synthetic cycles was not linear, e.g., membrane OL-15.5 showed an L_p value of 5.3±0.6 $L \cdot m^{-2}h^{-1}bar^{-1}$, which is close to that of membrane OL-20.5.

The permeance was inversely correlated with the number of oligoamide synthetic cycles (Fig. 2B); this correlation is in agreement with the inverse relation between the permeance of a membrane and the thickness of its barrier layer [39]. Hence, it implies that increased number of synthetic cycles led to higher oligoamide thickness, as observed in our previous study of

oligoamide synthesis on gold [40]. Additionally, the reduced permeance can be explained by the reduction in membrane pore volume and the subsequent increase in hydraulic resistance due to the oligoamide coating of the pores.

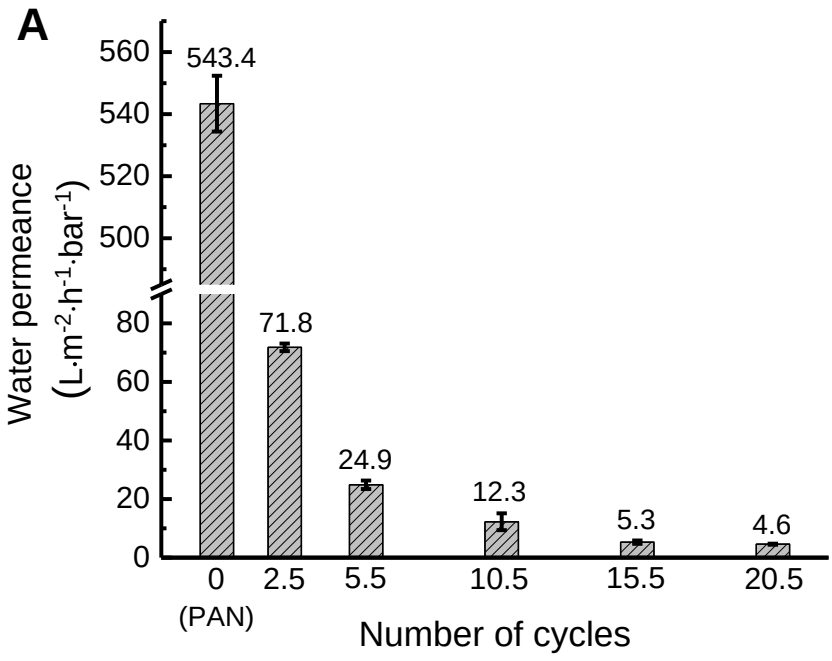

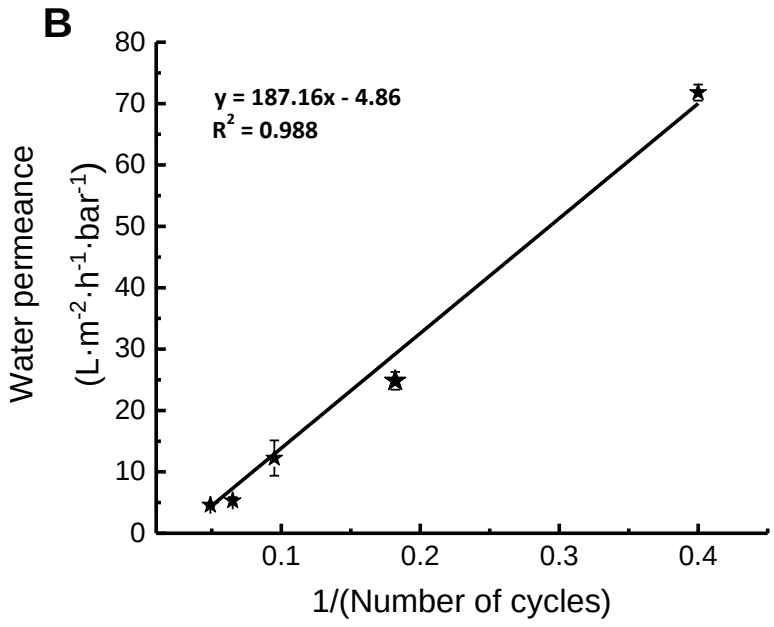

Figure 2. A) Water permeance (L_p) of membranes synthesized with 2.5, 5.5, 10.5, 15.5, and 20.5 cycles of oligoamide on aminated PAN support (5 h of amination), compared with pristine PAN membrane, and (B) the correlation between the water permeance and the inverse of number of synthetic cycles of oligoamide membranes.

To investigate the effect of the number of oligoamide synthetic cycles on the mean pore size of the membranes, MWCO values of the membranes were determined by filtration experiments using glucose, sucrose, PEG, and PEO as molecular markers. The solute rejection results are summarized in Fig. 3; it can be seen that higher number of oligoamide synthetic cycles resulted in higher solute rejection in all the range of molecular weights that were analyzed. Pristine PAN membrane showed the highest MWCO value of 332.0 kDa. Values for the OL-2.5, OL-5.5, OL-10.5, and OL-15.5 membranes were much lower (93.3, 92.0, 87.0, and 84.2 kDa, respectively), and the value for the OL-20.5 membrane was lower still (22.6 kDa). Note that the OL-15.5 and OL-20.5 membranes showed significant rejection of glucose and sucrose (MW of 180 and 342 g/mol, respectively; Fig. 3), which are small molecules. The mean pore sizes for all the membranes were calculated from the MWCO data according to the literature [33] and are presented in Fig. S1, Supporting Information. The pristine PAN membrane had the largest pores (24.1 nm), and the pores of the oligoamide membranes narrowed with the number of synthetic cycles to 0.4 nm for membrane OL-20.5 It should be noted that the standard deviations for membranes with high number of cycles were high (see Table S2 and Fig. S1, Supporting Information).

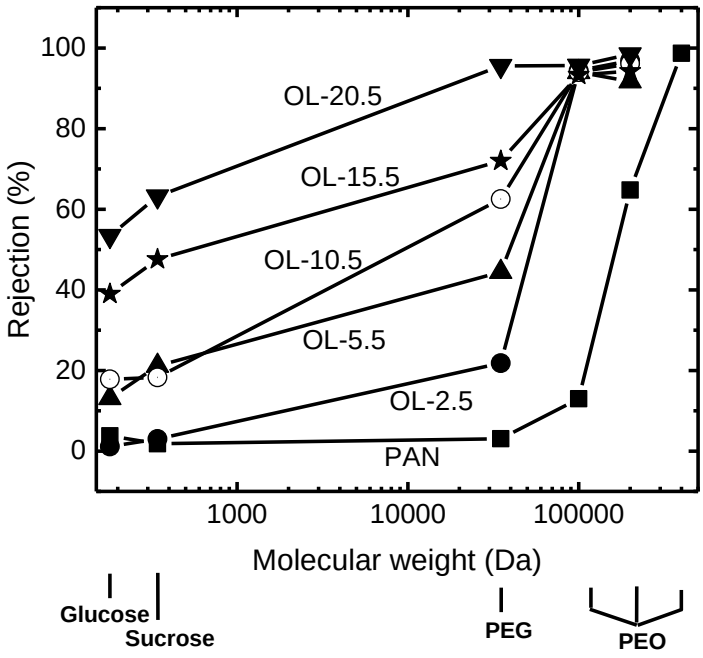

Figure 3. Rejection of polyethylene glycol (PEG), polyethylene oxide (PEO), glucose, and sucrose (solutions at 100 mg/L) by the oligoamide membranes in comparison with the pristine PAN membrane.

The separation performance of the oligoamide membranes was further tested by filtration experiments of rose bengal dye solutions. Filtration of 20 µM rose bengal solutions by the OL-2.5 and OL-5.5 membranes showed high rejection with good flux (Table 3). The OL-2.5 membrane showed a reasonable rose bengal retention of 78.6 ± 3.7% with a high flux of 194 ± 19.3 $L \cdot m^{-2}h^{-1}$ (at 3.5 bar) while the OL-5.5 membrane had a high rejection of 94.7 ± 0.5% and a flux of 126 ± 4.2$L \cdot m^{-2} \cdot h^{-1}$ (at 5.2 bar). The high retention for the negatively charged rose bengal with the OL-2.5 and OL-5.5 membranes having MWCO more than 90 kDa implies for the Donnan exclusion, probably due to the presence of charged carboxyl groups on the oligoamide surface which repels the negatively charged dye. Zeta potential analysis showed that OL-5.5 membrane is negatively charged in pH range of 4-9 (Fig. S2, Supporting Information). When comparing the rose bengal separation by the two oligoamide membranes, the higher rejection by the OL-5.5 membrane (compared to OL-2.5) can be explained by the increasing steric hindrance effect due to more synthetic cycles which is also evident in the water permeance data of the two membranes. The rose bengal dye separation performances obtained in this study for the oligoamide membranes were compared with other membranes that were recently published, and are summarized in Table S3 (Supporting Information). The permeability of OL-5.5 membrane is very high compared to most of the other membranes while maintaining a high retention of rose bengal (94.7%).

Table 3. Separation performance of rose bengal dye from water by OL-2.5 and OL-5.5 membranes.

Membrane	**Rose bengal rejection[a,b] (%)**	**Flux ($L \cdot m^{-2} \cdot h^{-1}$)**
PAN	14.7 ± 1.0	1158.8 ± 64.6 at 0.5 bar
OL-2.5	78.6 ± 3.7	194.9 ± 19.3 at 3.5 bar
OL-5.5	94.7 ± 0.5	126.4 ± 4.2 at 5.2 bar

a) Rose bengal molecular weight (of the di anion) is 973.67 g/mol.

b)

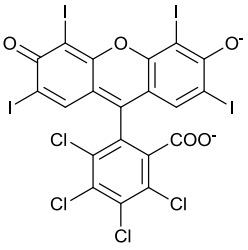

Rose bengal

The membranes were also examined for salt rejection (Fig. 4). All the oligoamide membranes rejected Na_2SO_4 at a higher rate than $MgSO_4$, suggesting the Donnan exclusion is an important mechanism of salt rejection by the membranes. Their salt rejection rates increased with increasing number of oligoamide synthesis cycles up to 15.5 cycles. Membrane OL-15.5 showed the highest rejection rates for both $MgSO_4$ and Na_2SO_4 (41.0% and 53.5%, respectively). Rejection rates then decreased in OL-20.5 to 34.1% and 43.5% for $MgSO_4$ and Na_2SO_4, respectively. The increased salt rejection with increasing number of oligoamide cycles may be explained by the smaller pores. Hence, the mechanism of salt rejection of the oligoamide membranes is a combination of both the Donnan exclusion, and the reduced pore size (size exclusion). Substantial ion rejection which was evident in the oligoamide membranes is not common for porous membranes, and this could represent a great advantage for the oligoamide membranes in the reclamation of wastewater for irrigation and in the separation of charged macromolecules. A small decrease in salt rejection for membrane OL-20.5 was noticed as compared with OL-15.5; however due to the very low permeance of OL-20.5 this membrane was not explored further.

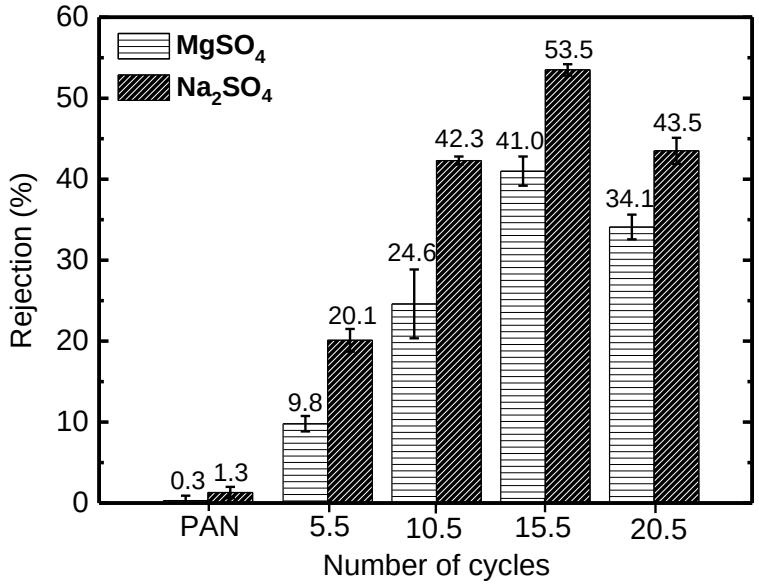

Figure 4. Rejection of Na_2SO_4 and $MgSO_4$ (1 g/L solutions) by oligoamide membranes and a pristine PAN membrane.

3.5. Microscopic characterization of membranes

The surface morphology of the various membranes was analyzed by SEM and is shown in Fig. 5A. The oligoamide membranes OL-5.5, OL-10.5, OL-15.5, and OL-20.5 appeared rough and porous, whereas the OL-2.5 membrane and the pristine PAN membrane had a smooth top surface. Hence, it is assumed that the fabricated oligoamide induces a rough-porous structure at the top surface, except for membrane OL-2.5 which had only 2.5 synthetic cycles.

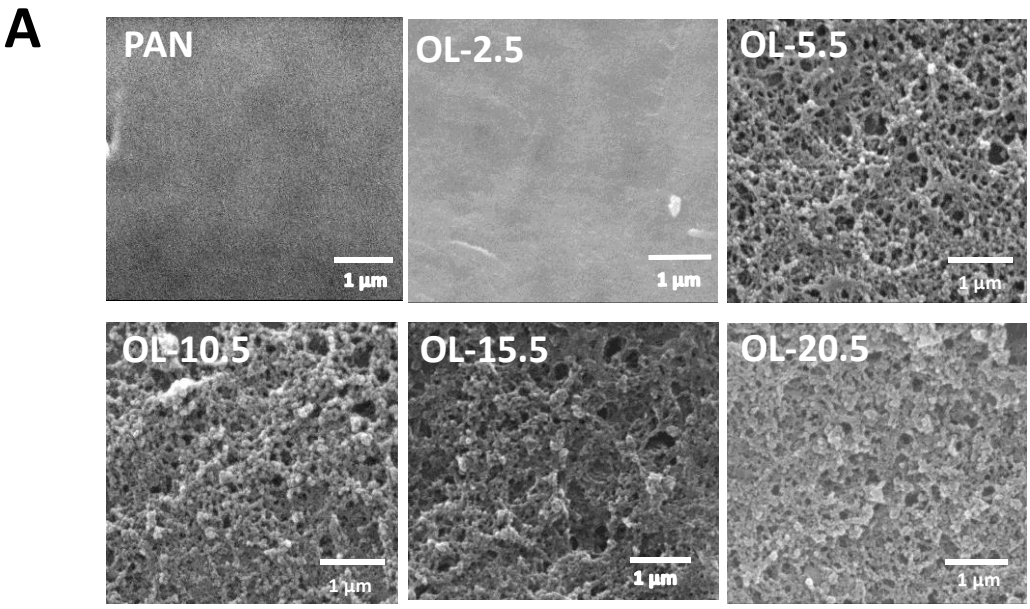

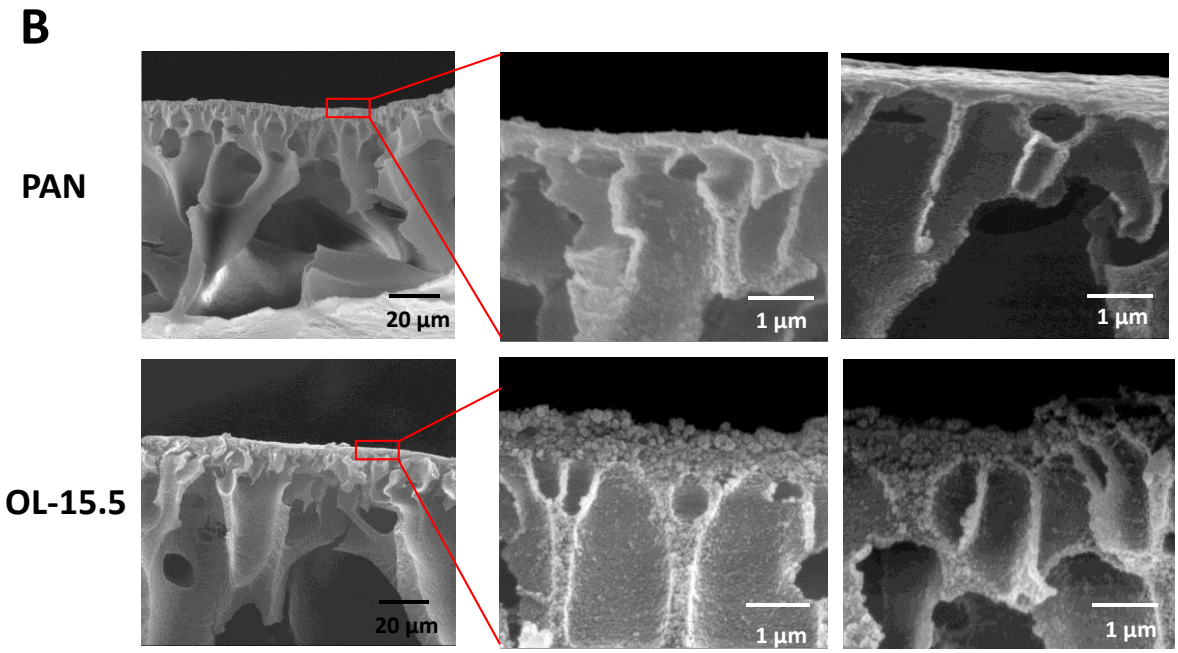

Figure 5. (A) SEM top surface images of a pristine PAN membrane and oligoamide membranes OL-2.5, OL-5.5, OL-10.5, OL-15.5, and OL-20.5. (B) Cross-sectional SEM images of the pristine PAN membrane (top) and oligoamide membrane OL-15.5 (bottom). Membranes shown in (A) were synthesized on commercial PAN supports, whereas those in (B) were synthesized on supports cast in the lab.

Cross-sectional SEM images were obtained for the OL-15.5 membrane and a pristine PAN membrane (Fig. 5B). Membrane OL-15.5 was chosen due to its interesting separation properties. Its synthesized oligoamide material appears as rounded features on top of the PAN support, as well as inside the membrane pores (Fig. 5B, high magnification). Based on that observation it is assumed that similar growth of oligoamide might also partly occur inside the small pores in the separating layer of the membrane, leading to decreased permeance and lower MWCO. There were no significant changes in the surface topology of the synthesized oligoamide membranes with the number of synthesis cycles. Overall, SEM analysis suggested that the oligoamide formed arbitrarily on the porous PAN support as rounded features on top of the surface, as well as inside the pores.

4. Conclusions

In this study, membranes with controllable MWCO and pore size were obtained by the stepwise synthesis of oligoamide on porous PAN supports. The technique relied on finding

an appropriate solvent (1,4-dioxane) for both coupling steps and washing steps, which was advantageous over the use of two different solvents. Another improvement in this synthesis was avoiding the use of a base in the TMC coupling stage. The formation of oligoamide on the membrane surface and the consequential control of its properties were demonstrated by different analysis techniques: Infrared spectroscopy showed the characteristic peaks of the amide functionality on the PAN support which increased with increasing number of synthesis cycles of oligoamide. In addition, the water permeance was inversely correlated with the number of oligoamide synthetic cycles. Furthermore, SEM analysis showed that the oligoamide formed as rounded features on the porous PAN support, at the surface and partly inside the pores.

Performance tests showed that the membranes' MWCO was controllable by varying the number of oligoamide synthetic cycles, from 332.0 kDa for the pristine membrane to 22.6 for the OL-20.5 membrane. Water permeance values ranged from 4.6±0.2 $L \cdot m^{-2} h^{-1} bar^{-1}$ for OL-20.5 membrane to 543.4±9.0 $L \cdot m^{-2} h^{-1} bar^{-1}$ for the pristine PAN membrane. The changes in MWCO and in the permeance may be explained by variations of the mean pore size, which varied from 0.4 nm of the OL-20.5 membrane to 23.5 nm for the pristine membrane. OL-2.5 and OL-5.5 membranes showed good separation of the charged rose bengal dye from water, with high water permeance (71.8 ± 1.3 $L \cdot m^{-2} \cdot h^{-1} \cdot bar^{-1}$ for OL-2.5 and 24.9 ± 0.8 $L \cdot m^{-2} \cdot h^{-1} \cdot bar^{-1}$ for OL-5.5) compared to some recently published membranes. Additionally, the oligoamide membranes could reject salts, showing maximum rejection rates of 41.0% for $MgSO_4$ and 53.5% for Na_2SO_4. As the oligoamide is covalently bonded to the support porous membrane, these membranes are expected to be more stable than other composite membranes (e.g., TFC nanofiltration or RO membranes) during membrane backwashing; therefore, they are expected to be more efficient and more durable in practice. The stepwise synthesis approach of oligoamide can be applied with organic porous supports other than PAN, given that an appropriate amination method and compatible solvents are found.

The oligoamide membranes described in this study may be used in applications that require control of the membrane transport properties, including the separation of charged macromolecules such as proteins with specific MWCO ranges, filtration of streams in the whey industry and in the pulp and paper industry, pharmaceutical separations, and hemodialysis.

Supporting Information contains the use of an organic base in oligoamide synthesis; details of PAN amination reaction; IR data of diethylenetriamine; the mean pore size and MWCO values of oligoamide membranes; zeta potential analysis of OL-5.5 and PAN membrane; and a comparison of the rose bengal separation performance of the oligoamide membranes with other membranes reported previously.

Acknowledgements

This work was supported by project "StepPolyMem" within the Italy–Israel Scientific and Technological Cooperation funded by the Ministry of Science, Technology and Space of the State of Israel and the Italian Ministry of Foreign Affairs and International Cooperation. We thank Yelena Logek (Ben-Gurion University of the Negev) for assisting with the lab work and Dr. Anya Milionchic and Roxana Golan (Ilse Katz Institute for Nanoscale Science, Ben-Gurion University of the Negev) for SEM analysis of the membranes. We thank professor Viacheslav (Slava) Freger (Technion – Israel Institute of Technology) for fruitful discussions.

References

[1] M.A. Shannon, P.W. Bohn, M. Elimelech, J.G. Georgiadis, B.J. Marinas, A.M. Mayes, Science and technology for water purification in the coming decades, Nature 452 (2008) 301-310.
[2] M. Elimelech, W.A. Phillip, The Future of Seawater Desalination: Energy, Technology, and the Environment, Science 333 (2011) 712-717.
[3] R.W. Baker, Membrane technology and applications, John Wiley & Sons, Ltd (2004) 96-103.
[4] T. Matsuura, Synthetic membranes and membrane separation processes, CRC press1993.
[5] S. Fakhfakh, S. Baklouti, S. Baklouti, J. Bouaziz, Preparation, characterization and application in BSA solution of silica ceramic membranes, Desalination 262 (2010) 188-195.
[6] L. Guo, L. Wang, Y. Wang, Stretched homoporous composite membranes with elliptic nanopores for external-energy-free ultrafiltration, Chem. Commun. 52 (2016) 6899-6902.
[7] I.M. Yamazaki, R. Paterson, L.P. Geraldo, A new generation of track etched membranes for microfiltration and ultrafiltration. Part I. Preparation and characterisation, J. Membr. Sci. 118 (1996) 239-245.
[8] R.J. Petersen, Composite reverse osmosis and nanofiltration membranes, J. Membr. Sci. 83 (1993) 81-150.
[9] A. Sarkar, P.I. Carver, T. Zhang, A. Merrington, K.J. Bruza, J.L. Rousseau, S.E. Keinath, P.R. Dvornic, Dendrimer-based coatings for surface modification of polyamide reverse osmosis membranes, J. Memb. Sci. 349 (2010) 421-428.
[10] V. Freger, J. Gilron, S. Belfer, TFC polyamide membranes modified by grafting of hydrophilic polymers: an FT-IR/AFM/TEM study, J. Membr. Sci. 209 (2002) 283-292.
[11] R. Malaisamy, A. Talla-Nwafo, K.L. Jones, Polyelectrolyte modification of nanofiltration membrane for selective removal of monovalent anions, Sep. Purif. Technol. 77 (2011) 367-374.
[12] W. Jin, A. Toutianoush, B. Tieke, Use of polyelectrolyte layer-by-layer assemblies as nanofiltration and reverse osmosis membranes, Langmuir 19 (2003) 2550-2553.
[13] J. Shi, W. Zhang, Y. Su, Z. Jiang, Composite polyelectrolyte multilayer membranes for oligosaccharides nanofiltration separation, Carbohydr. Polym. 94 (2013) 106-113.
[14] S.P. Nunes, A.R. Behzad, B. Hooghan, R. Sougrat, M. Karunakaran, N. Pradeep, U. Vainio, K.-V. Peinemann, Switchable pH-responsive polymeric membranes prepared via block copolymer micelle assembly, ACS Nano 5 (2011) 3516-3522.

[15] M. Sivakumar, D.R. Mohan, R. Rangarajan, Studies on cellulose acetate-polysulfone ultrafiltration membranes, J. Membr. Sci. 268 (2006) 208-219.
[16] A. Idris, L.K. Yet, The effect of different molecular weight PEG additives on cellulose acetate asymmetric dialysis membrane performance, J. Membr. Sci. 280 (2006) 920-927.
[17] Y.-H. Zhao, B.-K. Zhu, X.-T. Ma, Y.-Y. Xu, Porous membranes modified by hyperbranched polymers, J. Membr. Sci. 290 (2007) 222-229.
[18] B. Chakrabarty, A.K. Ghoshal, M.K. Purkait, Effect of molecular weight of PEG on membrane morphology and transport properties, J. Membr. Sci. 309 (2008) 209-221.
[19] M.V. Brami, Y. Oren, C. Linder, R. Bernstein, Nanofiltration properties of asymmetric membranes prepared by phase inversion of sulfonated nitro-polyphenylsulfone, Polymer 111 (2017) 137-147.
[20] R. Bernstein, E. Antón, M. Ulbricht, UV-Photo graft functionalization of polyethersulfone membrane with strong polyelectrolyte hydrogel and its application for nanofiltration, ACS Appl. Mater. Interfaces 4 (2012) 3438-3446.
[21] L. Yu, Y. Zhang, Y. Wang, H. Zhang, J. Liu, High flux, positively charged loose nanofiltration membrane by blending with poly (ionic liquid) brushes grafted silica spheres, J. Hazard. Mater. 287 (2015) 373-383.
[22] V. Vatanpour, N. Zoqi, Surface modification of commercial seawater reverse osmosis membranes by grafting of hydrophilic monomer blended with carboxylated multiwalled carbon nanotubes, Appl. Surf. Sci. 396 (2017) 1478-1489.
[23] K. Boussu, J. De Baerdemaeker, C. Dauwe, M. Weber, K.G. Lynn, D. Depla, S. Aldea, I.F.J. Vankelecom, C. Vandecasteele, B. Van der Bruggen, Physico-chemical characterization of nanofiltration membranes, ChemPhysChem 8 (2007) 370-379.
[24] S. Karan, Z. Jiang, A.G. Livingston, Sub–10 nm polyamide nanofilms with ultrafast solvent transport for molecular separation, Science 348 (2015) 1347-1351.
[25] M.R. Chowdhury, J. Steffes, B.D. Huey, J.R. McCutcheon, 3D printed polyamide membranes for desalination, Science 361 (2018) 682.
[26] Z. Steiner, J. Miao, R. Kasher, Development of an oligoamide coating as a surface mimetic for aromatic polyamide films used in reverse osmosis membranes, Chem. Commun. 47 (2011) 2384-2386.
[27] D. Wu, Y. Huang, S. Yu, D. Lawless, X. Feng, Thin film composite nanofiltration membranes assembled layer-by-layer via interfacial polymerization from polyethylenimine and trimesoyl chloride, J. Membr. Sci. 472 (2014) 141-153.
[28] W. Choi, J.-E. Gu, S.-H. Park, S. Kim, J. Bang, K.-Y. Baek, B. Park, J.S. Lee, E.P. Chan, J.-H. Lee, Tailor-made polyamide membranes for water desalination, ACS Nano 9 (2015) 345-355.
[29] J.-E. Gu, S. Lee, C.M. Stafford, J.S. Lee, W. Choi, B.-Y. Kim, K.-Y. Baek, E.P. Chan, J.Y. Chung, J. Bang, J.-H. Lee, Molecular layer-by-layer assembled thin-film composite membranes for water desalination, Adv. Mater. 25 (2013) 4778-4782.
[30] A. Amelio, M. Sangermano, R. Kasher, R. Bernstein, A. Tiraferri, Fabrication of nanofiltration membranes via stepwise assembly of oligoamide on alumina supports: Effect of number of reaction cycles on membrane properties, J. Membr. Sci. 543 (2017) 269-276.
[31] P.K. Neghlani, M. Rafizadeh, F.A. Taromi, Preparation of aminated-polyacrylonitrile nanofiber membranes for the adsorption of metal ions: Comparison with microfibers, J. Hazard. Mater. 186 (2011) 182-189.
[32] N. Nakajima, Y. Ikada, Mechanism of amide formation by carbodiimide for bioconjugation in aqueous media, Bioconjugate Chem. 6 (1995) 123-130.
[33] S. Singh, K.C. Khulbe, T. Matsuura, P. Ramamurthy, Membrane characterization by solute transport and atomic force microscopy, J. Membr. Sci. 142 (1998) 111-127.
[34] M. Ishiguro, T. Matsuura, C. Detellier, A Study on the Solute Separation and the Pore Size Distribution of a Montmorillonite Membrane, Sep. Sci. Technol. 31 (1996) 545-556.
[35] A.R. Cooper, D.S. Van Derveer, Characterization of Ultrafiltration Membranes by Polymer Transport Measurements, Sep. Sci. Technol. 14 (1979) 551-556.
[36] G. Hong, X. Li, L. Shen, M. Wang, C. Wang, X. Yu, X. Wang, High recovery of lead ions from aminated polyacrylonitrile nanofibrous affinity membranes with micro/nano structure, J. Hazard. Mater. 295 (2015) 161-169.
[37] P.M. Johnson, J. Yoon, J.Y. Kelly, J.A. Howarter, C.M. Stafford, Molecular layer-by-layer deposition of highly crosslinked polyamide films, J. Polym. Sci., Part B: Polym. Phys. 50 (2012) 168-173.
[38] Y. Zhao, Z. Zhang, L. Dai, H. Mao, S. Zhang, Enhanced both water flux and salt rejection of reverse osmosis membrane through combining isophthaloyl dichloride with biphenyl tetraacyl chloride as organic phase monomer for seawater desalination, J. Membr. Sci. 522 (2017) 175-182.
[39] V. Freger, Nanoscale heterogeneity of polyamide membranes formed by interfacial polymerization, Langmuir 19 (2003) 4791-4797.

581 [40] W. Ying, R. Kumar, M. Herzberg, R. Kasher, Diminished swelling of cross-linked aromatic oligoamide
582 surfaces revealing a new fouling mechanism of reverse-osmosis membranes, Environ. Sci. Technol. 49 (2015)
583 6815-6822.

584